



# **MICROWAVE-ASSISTED SYNTHESIS OF ZnO NANOPARTICLES FROM 1, 2, 3 TRI SUBSTITUTED IONIC LIQUID AND THEIR ANTIMICROBIAL AND BIOFILM ACTIVITIES**

**K. SARAVANAN and K. RAJATHI\***

P.G and Research Department of Chemistry, Govt. Arts College, THIRUVANNAMALAI (T.N.) INDIA

## **ABSTRACT**

In the present investigation, certain highly substituted imidazolium based ionic liquids ([HEMIM] BF<sub>4</sub> and [HEMIM] PF<sub>6</sub>) were synthesized and the structures were confirmed by spectral studies such as FT-IR, <sup>1</sup>H-NMR and <sup>13</sup>C-NMR. Stable zinc oxide nanoparticles were successfully synthesized by wet chemical method using imidazolium based ionic liquids (ILs). The structural, morphological and chemical composition of the nanoparticles have been investigated by X-Ray Diffraction (XRD), Scanning Electron Microscopy (SEM) and with Energy Dispersive X-ray spectroscopy (EDX). The antimicrobial activity of the zinc oxide (ZnO) nanoparticles were studied by determining its minimum inhibitory concentration (MIC) by broth dilution method and bio film inhibition of ZnO were also tested against one gram positive and one gram negative bacteria. In view of the results, it appeared that nanoparticles prepared in ionic liquids with PF<sub>6</sub><sup>-</sup> are the most effective products against the tested bacterial strains compared with nanoparticles prepared in ionic liquids with BF<sub>4</sub><sup>-</sup> anion.

**Key words:** Zinc oxide, Nanoparticles, Microwave synthesis, Antimicrobial, Biofilm inhibition.

## **INTRODUCTION**

Ionic liquids have been generating increasing interest over the last decade. Ionic liquids have become interesting alternatives to traditional solvents and are intensively investigated as new liquid media for synthesis and catalysis<sup>1-3</sup>. ILs may offer morphology control of materials. Room-temperature ionic liquids (ILs) are attractive environmentally benign solvents for organic chemical reactions, separations, and electrochemical applications<sup>4</sup>. Particularly, ionic liquids can act as solvents, reactants and templates for the fabrication of inorganic materials. Nanoparticles represent a significant category of

---

\* Author for correspondence; E-mail: rajathi\_sridhar@rediffmail.com

nanomaterials. Nanoparticles are of nice scientific interest as a result of the exhibit distinctive, fascinating electronically, optical and biological properties and are a perfect size to be used as nanotechnological building blocks.

Zinc oxide has been famous for a wide range of applications in the functional devices, photo-catalysts, optical materials, cosmetics, nanostructure varistors, UV absorbers and gas sensors<sup>5,6</sup>. Various applications exist for ZnO including solar energy conversion, sensors, catalyst, piezoelectric transducers, actuators, batteries, antimicrobial agent and drug delivery systems<sup>7</sup>. One of the most important environmental applications of nanomaterials is their use as sensors with enhanced monitoring capabilities for pollutants. They are used for treating contaminated water, soil or air and in green technologies to eliminate or decrease harmful emissions and wastes from industry using photo catalytic processes. The considerable antimicrobial activities of inorganic metal oxide nanoparticles such as ZnO, MgO, TiO<sub>2</sub>, SiO<sub>2</sub> and their selective toxicity to biological systems suggest their potential application as therapeutics, diagnostics, surgical devices and nanomedicine based antimicrobial agents<sup>8-10</sup>. The advantages of using these inorganic oxides nanoparticles as antimicrobial agents are their greater effectiveness on resistant strains of microbial pathogens, less toxicity and heat resistance. In addition, they provide mineral elements essential to human cells and even small amounts of them exhibit strong activity<sup>11</sup>. The size and morphology of ZnO nanoparticles have great influences on their performances and applied aspects. In this paper, we report an effective method for the preparation of ZnO nanoparticles by using microwave irradiation. In recent years, the microwave method has been rapidly developed for synthesis of nanomaterial. Ionic liquids are excellent microwave absorbing agents due to their high ionic conductivity and polarizability, thus leading to a high heating rate and a significantly shortened reaction time<sup>12</sup>. The microwave irradiation method considered herein is fast, mild, energy-efficient, and environment-friendly. Hence, it is not a weak substitute of the conventional method.

## EXPERIMENTAL

### Materials and methods

All the reagents used in this research are of analytical grade. Synthesized ionic liquids was characterized by <sup>1</sup>H-NMR and <sup>13</sup>C-NMR spectra were recorded in CDCl<sub>3</sub> and DMSO-d<sub>6</sub> on a Joel JNN ECX 400P spectrometer. The FT – IR spectra were obtained on a Varian 800 FT-IR as thin films or for solid samples. Nanoparticles were well characterized by powder X-ray diffraction (powder XRD), Scanning Electron Microscope (SEM) and EDX analysis. The X-ray diffraction (XRD) patterns were recorded on a Philips Xpert X-ray diffractometer with Cu K $\alpha$  radiation ( $\lambda = 0.15406$  nm) employing a scan rate of 1<sup>o</sup>/min in the

2 $\theta$  range from 20° to 80°. Surface morphology and the distribution of particles were characterized by a LEO 1430VP scanning electron microscopy (SEM) using an accelerating voltage of 15 kV.

### Synthesis of ionic liquids

1-hexyl-3-methylimidazolium bromide [HMIM] Br, 1-hexyl-2-ethyl-3-methylimidazolium bromide [HEMIM] Br, 1-hexyl-2-ethyl-3-methylimidazolium tetrafluoroborate [HEMIM] BF<sub>4</sub>, 1-hexyl-2-ethyl-3-methylimidazolium hexafluorophosphate [HEMIM] PF<sub>6</sub> ILs was prepared according to the published method<sup>13-15</sup>. The product was characterized by FT-IR, <sup>1</sup>H - NMR and <sup>13</sup>C NMR spectral studies.

#### Characterization of 1-hexyl-3-methylimidazolium bromide [HMIM]Br

FT-IR (neat): 3,153, 3,102, 2,990, 2,878, 2,833, 2,078, 1,633, 1,571, 1,457, 1388, 1301, 1,022, 842, 760, 619, 523 cm<sup>-1</sup>; <sup>1</sup>H NMR:  $\delta$  1.41 (t, J = 7.3, 3H), 3.85 (s, 3H), 4.14 (q, J = 7.3, 2H), 7.35 (s, 1H), 7.41 (s, 1H), 8.55 (s, 1H); <sup>13</sup>C NMR:  $\delta$  15.2, 36.0, 45.1, 122.2, 123.8, 135.9.

#### Characterization of 1-hexyl-2-ethyl-3-methylimidazolium bromide [HEMIM] Br

FT-IR (neat): 3407, 3158, 2996, 2878, 1659, 1580, 1533, 1462, 1388, 1289, 1236, 1066, 842, 760, 619, 523 cm<sup>-1</sup>; <sup>1</sup>H NMR:  $\delta$  7.79 (s, 1H), 7.602 (s, 1H), 4.35 (t, 2H), 4.41 (m, 2H), 3.71 (m, 2H), 1.94 (m, 6H), 1.38 (m, 2H), 0.91 (s, 3H); <sup>13</sup>C NMR:  $\delta$  146.68, 136.01, 122.79, 49.28, 36.09, 30.48, 29.62, 25.34, 21.69, 16.72, 13.28, 11.02.

#### Characterization of 1-hexyl-2-ethyl-3-methylimidazolium tetrafluoroborate [HEMIM] BF<sub>4</sub> [IL-1]

FT-IR (neat): 3456, 3326, 2296, 1649, 1513, 1427, 1355, 1054, 1026, 828, 730, 619 cm<sup>-1</sup>; <sup>1</sup>H NMR:  $\delta$  7.48 (s, 1H), 7.36 (s, 1H), 4.22 (t, 2H), 3.95 (m, 2H), 3.06 (m, 2H), 1.86 (m, 6H), 1.03 (m, 2H), 0.86 (s, 3H); <sup>13</sup>C NMR:  $\delta$  135.58, 120.52, 49.42, 35.66, 30.61, 29.65, 25.25, 21.84, 16.20, 13.41, 10.75.

#### Characterization of 1-hexyl-2-ethyl-3-methylimidazolium hexafluorophosphate [HEMIM] PF<sub>6</sub> [IL-2]

FT-IR (neat): 3453, 2095, 1638, 1587, 1450, 1337, 1176, 1067, 859, 787, 583 cm<sup>-1</sup>; <sup>1</sup>H NMR:  $\delta$  8.4 (s, 1H), 7.26 (s, 1H), 4.15 (t, 2H), 3.88 (m, 2H), 3.05 (m, 2H), 1.82 (m, 6H), 1.31 (m, 2H), 0.89 (s, 3H); <sup>13</sup>C NMR:  $\delta$  135.71, 122.84, 50.02, 48.40, 34.81, 31.10, 25.89, 22.53, 16.61, 13.89, 11.12.

### **Synthesis of zinc oxide nanoparticles**

Zinc acetate dihydrate (5.5 g) was dissolved in 50 mL of distilled water, and then solid sodium hydroxide (16 g) was slowly added into the solution under magnetic stirring at room temperature, and formed a transparent  $[\text{Zn}(\text{OH})_4]^{2-}$  solution. Then 2 mL of IL was added to 3 mL of the above solution. The suspension was put into a domestic microwave oven in air, 30% of the output power of the microwave was used to irradiate the mixture for 2-9 min in a cycling mode (on: 10s, off: 5s)<sup>16</sup>. The white precipitate was separated by centrifugation, washed with deionized water and ethanol several times, and dried in vacuum oven at 40°C for 10 h.

### **Antimicrobial activity (Broth dilution assay)**

A series of fifteen test tubes were filled with 0.5 mL sterilized nutrient broth. Sequentially, test tubes 2-14 received an additional 0.5 mL of the sample serially diluted to create a concentration sequence from 500-0.06 µg. The first test tube served as the control. All the test tubes received 0.5 mL of inoculums. The test tubes were vortexed well and incubated for 24 h at 37°C. The resulting turbidity was observed, and after 24 h the Minimum Inhibition Concentration (MIC) was determined where growth was no longer visible by assessment of turbidity by optical density readings at 600 nm<sup>17</sup>.

### **Biofilm formation inhibition of pathogenic bacteria**

Effect of nanoparticle on biofilm formation a modified microtitre plate assay was performed to see the effect alkaloid extract on pathogenic bacteria biofilm formation. In brief, sterile, polystyrene microtitre plate wells were inoculated with 100 µL nutrient broth containing  $10^7$  CFU/mL and loaded with different concentrations of alkaloid extract (5-20 µg/mL). These plates were incubated in static condition at 37°C for 24 h. Controls wells were maintained with medium containing bacterial suspension. Then, medium in the wells was removed and washed with sterile phosphate buffer saline to remove loosely attached bacteria. Wells were stained with 150 µL of 0.25% crystal violet and incubated for 30 min<sup>18</sup>. Further these wells were washed, air dried, bound stain was solubilized in 150 µL of 95% ethanol and the absorbance at 595 nm was recorded using the plate reader.

## **RESULTS AND DISCUSSION**

### **XRD analysis**

The phase, purity and crystallite size of the ZnO nanoparticles synthesized in IL-1 were studied by XRD (Fig. 1a). Based upon peak width, the diffractions assigned to ZnO nanostructure products have been de-convoluted where it can be observed that they are in

agreement with the diffraction patterns of neat high crystalline ZnO, with a hexagonal, primitive structure (JCPDS 36-1451). In addition to identification of the crystalline phases, XRD data were used to estimate size of the constituent crystallites by Scherrer equation<sup>19</sup>. The average particle size,  $D$ , was determined using  $D = K \lambda / \beta \cos\theta$  Where,  $\lambda$  is the wavelength of X-ray radiation (0.15406),  $K$ , the Scherrer's constant ( $K = 0.9$ ),  $\theta$  the characteristic X-ray radiation ( $2\theta = 29.4$ ) and  $\beta$  is the fullwidth-half-maximum of the (100) plane (in radians). According to the full width at half maximum of the diffraction peaks, the average size of the particles could be estimated from the Scherrer equation to be about 35.79 nm.

Fig. 1b is the powder X-ray diffraction patterns of the ZnO nano products prepared in IL-2. The diffraction patterns and interplane spacings can be well matched to the standard diffraction pattern of wurtzite ZnO, demonstrating the formation of wurtzite ZnO nanocrystals. According to the full width at half maximum of the diffraction peaks, the average size of the particles could be estimated from the Scherrer equation to be about 41.9 nm.

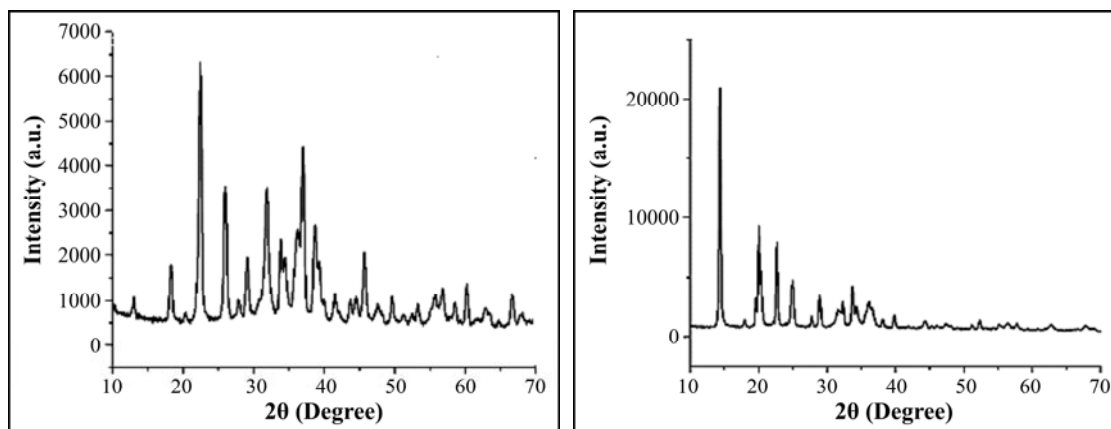


**Fig. 1: The XRD pattern of ZnO nanoparticle in [HEMIM] BF<sub>4</sub> and [HEMIM] PF<sub>6</sub>**

Not only the size of the particles, but also the crystallite size of ZnO samples prepared with different ionic liquids deviates from one to one, suggesting that an each ionic liquid (same cation with different anion) has different nanostructures in certain direction of the growing material. Anion plays an important role for fabricating different nanostructures.

### SEM analysis

Morphology of the as synthesized ZnO nanoparticles in two different ILs was investigated by scanning electron microscope (SEM) recorded at different magnifications. Fig. 2a and 2b shows the SEM image of ZnO nanoparticle assisted by [HEMIM] BF<sub>4</sub> and

[HEMIM] PF<sub>6</sub> respectively. Ionic liquids are particularly interesting species in green chemistry not only as they can act as template to control the particle shape and assembly behavior, but also their ionic properties can drastically enhance the efficiency of the nanoparticle production.

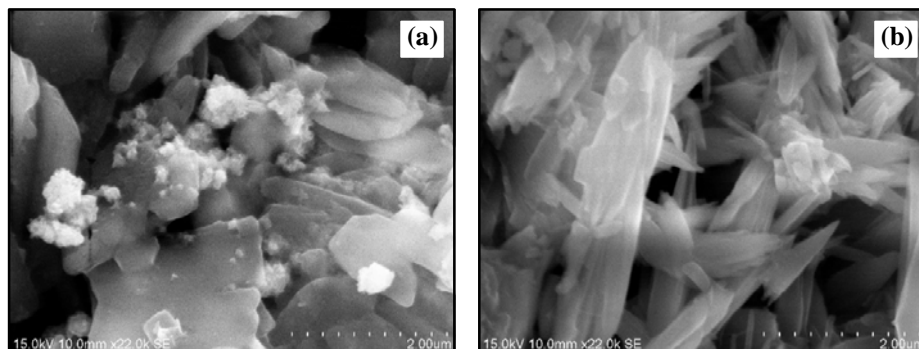
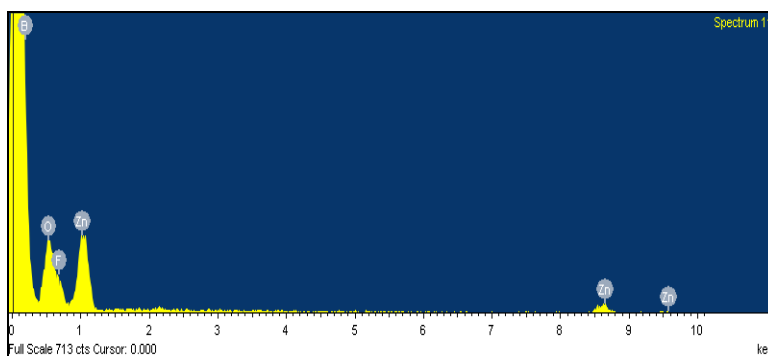


**Fig. 2: SEM image of ZnO nanoparticles in [HEMIM] BF<sub>4</sub> and [HEMIM] PF<sub>6</sub>**

It is evident from the Fig. 2a that the synthesized ZnO particles from IL1 exhibit the morphology of flakes shaped particles. When the anion PF<sub>6</sub><sup>-</sup> is introduced instead of BF<sub>4</sub><sup>-</sup>, the morphology and size of ZnO also tuned as flower-like shaped particles (Fig. 2(b)). When the PF<sub>6</sub><sup>-</sup> anion is introduced, the synthesized ZnO particles size is constricted due to the high coordination, chunkiness of the particle decreases from flakes to flower like.

### EDX pattern of ZnO nanoparticle

The purity and composition of the products nanoparticles in [HEMIM] BF<sub>4</sub> and [HEMIM] PF<sub>6</sub> were studied by energy dispersive X-ray spectroscopy (EDX). The results are displayed in Fig. 3a-b.



Cont...

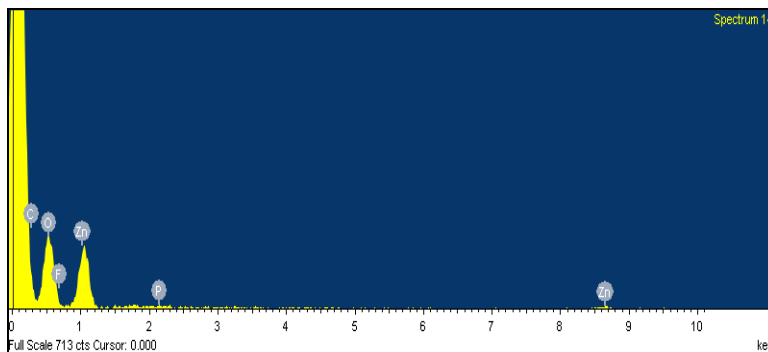


**Fig. 3: EDX pattern of ZnO nanoparticles in [HEMIM] BF<sub>4</sub> and [HEMIM] PF<sub>6</sub>**

The other peaks in the figure corresponded to gold, palladium, and silicate which were due to sputter coating of the glass substrate on the EDX stage and these were not considered in the elemental analysis of ZnO nanoparticle. It is clear that the ZnO nanoparticles prepared was sufficiently pure.

### Antimicrobial activity of ZnO nanoparticle

Antibacterial activity of the ZnO nanostructures was investigated against one gram positive bacteria (*Staphylococcus aureus*) and one gram negative bacteria (*Pseudomonas aeruginosa*) by broth dilution method. ZnO inactivation of bacteria involves the direct interaction between ZnO nanoparticles and cell surfaces, which affects the permeability of membranes where nanoparticles enter and induce stress in bacterial cells, subsequently resulting in the inhibition of cell growth and eventually in cell death.

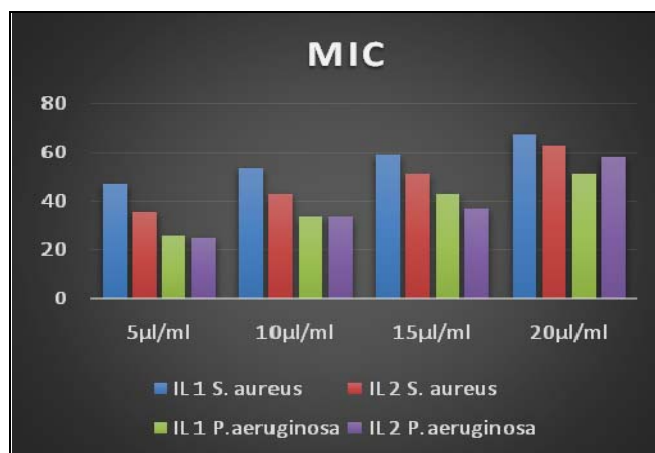


**Fig. 4: Comparison of MIC values of ZnO nanoparticles in [HEMIM] BF<sub>4</sub> and [HEMIM] PF<sub>6</sub>**

In view of the results, it appeared that in both the pathogens antimicrobial activity increases with increase in concentrations. Nanoparticles synthesized in ionic liquids with  $\text{PF}_6^-$  are the most effective products against the tested bacterial strains compared with nanoparticles prepared in ionic liquids with  $\text{BF}_4^-$  anion. Compared with two different microorganism gram negative bacteria is more effective than positive gram bacteria (Fig. 4).

### Effect synthesized particles on inhibition of biofilm formation on pathogenic bacteria

Static biofilm quantification assay was performed to evaluate the effect of ZnO nanoparticles in IL-1 and in IL-2 on *S. aureus* and *P. aeruginosa* biofilm formation. Fig. 5 shows the difference in biofilm formation between the control (i.e., no particles addition) and the culture containing particles (5, 10, 15 and 20  $\mu\text{g}/\text{mL}$ ). The microtiter plates showed that biofilm formation for the experimental group (i.e. cultures with synthesized particles) was 39-56% less than the amount of formation in the control. The results suggested that the biofilm formation of both the bacteria were inhibited by the addition of synthesized ZnO in IL1 and in IL2 particles in microtiter plates.

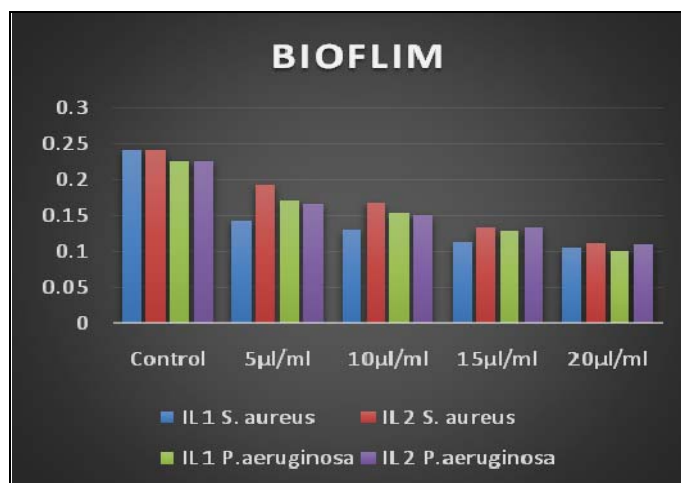


**Fig. 5: Comparison Biofilm formation of ZnO nanoparticles in [HEMIM]  $\text{BF}_4$  and [HEMIM]  $\text{PF}_6$**

### ACKNOWLEDGEMENT

The authors thank the Principal and Department of Government Arts College, Thiruvannamalai for the constant encouragement and support rendered.



## REFERENCES

1. P. Wasserscheid and W. Keim, Ionic Liquids – New "Solutions" for Transition Metal Catalysis, *Angew Chem. Int. Ed.* (2000).
2. V. I. Parvulescu and C. Hardacre, *Chem. Rev.*, **107**, 2615 (2007).
3. P. Lodge, *Science*, **321**, 50 (2008).
4. R. Sheldon, *Chem. Communication*, 2399 (2001).
5. M. R. Vaeziand and S. K. Sadrnezhaad, *Materials and Design*, **28**, 515 (2007).
6. Y. J. Kwon, K. H. Kim, C. S. Lim and K. B. Shim, *J. Ceramic Proc. Res.*, **3**, 146 (2002).
7. S. Selvam, R. Rajiv Gandhi, J. Suresh, S. Gowri and M. Sundrarajan, *Int. J. Pharm.*, **434**, 366 (2012).
8. K. A. Laura, L. Delinay and J. A. Pedro, *J. Water Res.*, **40**, 3527 (2006).
9. J. Sawai and T. Yoshikawa, *J. Microb Meth.*, **54**, 177 (2003).
10. K. M. Reddy, F. Kevin, B. Jason, G. W. Denise, H. Cory and P. Alex, *J. Appl. Phys. Lett.*, **90**, 1 (2007).
11. Z. A. Zakaria, A. Matdesa, K. Ramasamy, N. Ahmat, A. S. Mohamad, D. A. Israf and M. R. Sulaiman, *Afr. J. Microbial Res.*, **4**, 71 (2010).
12. P. Wasserscheid and T. Welton, *Ionic Liquids in Synthesis*, Wiley-VCH, Weinheim (2008).
13. E. Ennis and S. T. Handy, *Molecules*, **14**, 2235 (2009).
14. K. Rajathi and A. Rajendran, *Research and Reviews: J. Chem.*, **2**, 36 (2013).
15. S. Park and R. J. Kazlauskas, *J. Org. Chem.*, **66**, 8395 (2001).
16. K. Elaheh, K. Goharshadi, Y. Ding, X. Lai and P. Nancarrow, *Inorg. Mater.*, **47**, 379 (2011).
17. A Brantner and E. Grein, *J. Ethnopharmacol.*, **44**, 35 (1994).
18. D. Djordjevic, M. Wiedmann and L. A. McLandsborough, *Appl. Environ. Microbiol.*, **68**, 2950 (2002).
19. B. D. Cullity, *Elements of X-Ray Diffraction*, 2<sup>nd</sup> Ed., Addison Wesley, London (1978).

*Accepted : 25.11.2016*